Effective Permittivity of Mixtures: Numerical Validation by the FDTD Method

Kimmo Kalervo Kärkkäinen, Ari Henrik Sihvola, and Keijo I. Nikoskinen

***Abstract*—The present paper reports the results of an extensive numerical analysis of electromagnetic fields in random dielectric materials. The effective permittivity of a two-dimensional (2-D) dielectric mixture is calculated by FDTD simulations of such a sample in a TEM waveguide. Various theoretical bounds are tested in light of the numerical simulations. The results show how the effective permittivity of a mixture with random inclusion positionings is distributed. All possible permittivity values lie between Wiener limits, and according to FDTD simulations the values are almost always between Hashin-Shtrikman limits. Calculated permittivity distribution is also compared with theoretical mixture models. No model seems to be able to predict the simulated behavior over the whole range of volume fraction.**

***Index Terms*—Effective permittivity, FDTD, mixing rules.**

I. Introduction

In an earlier paper [1], we presented a way to calculate numerically the effective dielectric constant of a random mixture. The mixture was two-dimensional (2-D). In other words, the randomness of the structure was limited to a plane, and along the third dimension, the geometry would not vary. The mixture was a two-component mixture with a homogeneous background in which circles of another material were embedded in random positions. The circles were allowed to touch and overlap, which means that the mixture also contained more complex cluster geometries than the 2-D spheres.

The result of the study was that the effective permittivity of the simulated mixtures fell between the predictions of two classical mixing rules: the Maxwell Garnett formula and the Bruggeman formula. Of course, every new simulation of the random medium is individually different even if they have the same volume proportions of the phases, and hence a variation is to be expected in the results. In theoretical modeling of random media, not only predictions for the permittivity of a mixture have been given but also bounds between which the permittivity should be. The aim of the present study is to test how well these bounds are valid, in light of the numerically solved effective permittivities for the simulated mixtures. Each mixture is solved numerically by the FDTD method.

The results bear hopefully statistical significance because the number of simulations is thousands. In addition to studying the way how the results of a large number of simulations fall between the predicted bounds, we also test the validity of a class of so-called exponential mixing formulas and ν-models. Although many numerical studies have been performed to analyze the effective response of mixtures [2]–[4], we believe that our approach is the first that applies the dynamical solution method (FDTD) for this quasistatic problem.

Manuscript received March 25, 1999; revised September 2, 1999

The authors are with the Helsinki University of Technology (HUT), Espoo, Finland (e-mail: kimmo@eml.hut.fi).

Publisher Item Identifier S 0196-2892(00)02852-7.

II. Two-Dimensional (2-D) Mixing Models

As mentioned previously, we limit the attention in the following to 2-D mixtures. Also, the mixture consists of two dielectric components, of which one is treated as host and the other as the inclusion phase. In the literature, many mixing models can be found for the effective dielectric permittivity of such a mixture. Here we present only some.

For the case of circular inclusions, the prediction of the effective permittivity of the mixture ϵ_{eff} according to the Maxwell Garnett mixing rule reads [1] [5], [6]

$$\epsilon_{\text{eff}} = \epsilon_e + 2f\epsilon_e \frac{\epsilon_i - \epsilon_e}{\epsilon_i + \epsilon_e - f(\epsilon_i - \epsilon_e)} \tag{1}$$

Here, circular cylinders (2-D spheres) of permittivity ϵ_i are located randomly in a homogeneous environment (ϵ_e) and occupy a volume fraction f. The quasistatic nature of the mixture means that the wavelength of the field is much larger than the inclusion diameter.

Another famous mixing rule is the Bruggeman formula [7]

$$(1-f)\frac{\epsilon_e - \epsilon_{\text{eff}}}{\epsilon_e + \epsilon_{\text{eff}}} + f\frac{\epsilon_i - \epsilon_{\text{eff}}}{\epsilon_i + \epsilon_{\text{eff}}} = 0 \tag{2}$$

In remote sensing studies, Bruggeman rule is perhaps better known as Polder–van Santen formula [8]. The mixing approach presented in [9] collects dielectric mixing rules into one family

$$\frac{\epsilon_{\text{eff}} - \epsilon_e}{\epsilon_{\text{eff}} + \epsilon_e + \nu(\epsilon_{\text{eff}} - \epsilon_e)} = f\frac{\epsilon_i - \epsilon_e}{\epsilon_i + \epsilon_e + \nu(\epsilon_{\text{eff}} - \epsilon_e)} \tag{3}$$

This formula contains a dimensionless parameter ν. For different choices of ν, the previous mixing rules are recovered. $\nu = 0$ gives the Maxwell Garnett rule, $\nu = 1$ gives the Bruggeman formula, and $\nu = 2$ gives the Coherent potential [10], [11] approximation.

In modeling analysis, quite often power-law models are used. These give the effective permittivity of the mixture as

$$\epsilon_{\text{eff}}^{\beta} = f\epsilon_i^{\beta} + (1-f)\epsilon_e^{\beta} \tag{4}$$

where β is a dimensionless parameter. Known examples are the Birchak formula $(\beta = 1/2)$ [12] and Looyenga formula $(\beta = 1/3)$ [13]. Also, the Lichtenecker formula [14]

$$\ln \epsilon_{\text{eff}} = f \ln \epsilon_i + (1-f)\ln \epsilon_e \tag{5}$$

is a special case of the power-law models, for the limit $\beta \to 0$.

[1] In the present paper, the permittivity ϵ is a *relative* quantity compared to the free-space permittivity $\epsilon_0 = 8.854 \cdot 10^{-12}$ F/m.

0196–2892/00$10.00 © 2000 IEEE

III. Theoretical Bounds for the Effective Permittivity

Different mixing models predict different effective permittivity values for a given mixture. However, there are bounds that limit the range of the predictions. The loosest bounds are the so-called Wiener bounds [15]. These effective permittivity bounds are

$$\epsilon_{\text{eff,max}} = f\epsilon_i + (1-f)\epsilon_e \tag{6}$$

and

$$\epsilon_{\text{eff,min}} = \frac{\epsilon_i\epsilon_e}{f\epsilon_e + (1-f)\epsilon_i} \tag{7}$$

These two cases correspond to capacitors that are connected in parallel or series in a circuit. It is worth noting also that these two cases are the effective permittivities from the mixing formulas with aligned ellipsoids, where the depolarization factors are 0 and 1, respectively. Note that the bounds retain the minimum and maximum character independently of the type of the mixture, in other words (6) is the maximum for both $\epsilon_i > \epsilon_e$ and $\epsilon_i < \epsilon_e$. Also, (7) is the minimum for both cases.

For a statistically homogeneous and isotropic mixture, other bounds have been generally accepted in the literature [16]. The following Hashin-Shtrikman bounds are based on a variational treatment of the energy functional for the mixture where the inhomogeneity is distributed in three dimensions

$$\epsilon_{\text{eff,min}} = \epsilon_e + \frac{f}{\frac{1}{\epsilon_i-\epsilon_e} + \frac{1-f}{3\epsilon_e}} \tag{8}$$

and

$$\epsilon_{\text{eff,max}} = \epsilon_i + \frac{1-f}{\frac{1}{\epsilon_e-\epsilon_i} + \frac{f}{3\epsilon_i}} \tag{9}$$

where it is assumed that $\epsilon_e < \epsilon_i$. For a 2-D mixture, the bounds would read

$$\epsilon_{\text{eff,min}} = \epsilon_e + \frac{f}{\frac{1}{\epsilon_i-\epsilon_e} + \frac{1-f}{2\epsilon_e}} \tag{10}$$

and

$$\epsilon_{\text{eff,max}} = \epsilon_i + \frac{1-f}{\frac{1}{\epsilon_e-\epsilon_i} + \frac{f}{2\epsilon_i}} \tag{11}$$

Note that the lower limit is in fact exactly the Maxwell Garnett mixing rule, and the upper limit is the Maxwell Garnett prediction for the "complementary" mixture. A complementary mixture emerges with the change $\epsilon_i \to \epsilon_e$, $\epsilon_e \to \epsilon_i$, $f \to 1-f$.

IV. Principle of Numerical Calculation

The effective permittivity of a mixture is determined by calculating the reflection from a sample. The sample is put in a TEM waveguide and fields are solved by the FDTD method. The sample is composed of host material and randomly positioned circular inclusions. Clustering of inclusions is allowed which means that inclusions can form connected sets when overlapping each other. The size distribution of the inclusions need not be uniform, but all particles have to be within the quasistatic limit. However, from numerical analysis point of view, it is convenient to have a constant radius of inclusion. Hence, the inclusion volume fraction is controlled with the number of inclusions. Fig. 1 illustrates the simulation setup. The voltage pulse is excited to travel in the waveguide and the reflected pulse is observed.

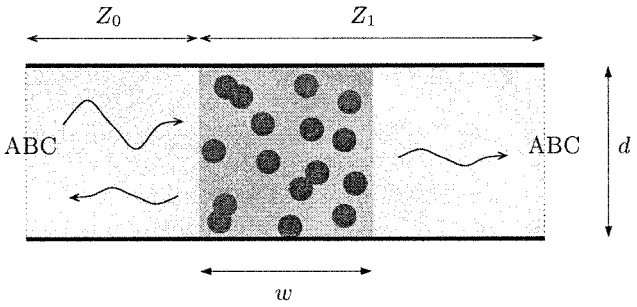

Fig. 1. Mixture sample in TEM-waveguide.

With the help of transmission line theory, the effective permittivity can be determined. Based on the transmission line theory, the absolute value of the reflection coefficient acting at the left boundary of the slab is

$$|R| = \left|\frac{Z_1 - Z_0}{Z_1 + Z_0}\right| \tag{12}$$

where Z_0 is free space impedance $\sqrt{\mu_0/\epsilon_0}$ (this is also applicable to the TEM waveguide), and Z_1 is the "input impedance" of the slab/free space system. If the width of the slab is w and effective relative permittivity is ϵ_{eff}, then

$$Z_1 = Z_0\frac{1 + j\epsilon_{\text{eff}}^{-1/2}\tan(kw)}{1 + j\epsilon_{\text{eff}}^{1/2}\tan(kw)} \tag{13}$$

where $k = (\omega/c_0)\epsilon_{\text{eff}}^{1/2}$ and ω is angular frequency, and c_0 is the velocity of light in a vacuum. From (12) and (13), one obtains the following transcendental equation for the effective relative permittivity

$$|R| + \frac{\tan\left(\frac{\omega w}{c_0}\epsilon_{\text{eff}}^{1/2}\right)(\epsilon_{\text{eff}} - 1)}{\sqrt{4\epsilon_{\text{eff}} + \tan^2\left(\frac{\omega w}{c_0}\epsilon_{\text{eff}}^{1/2}\right)(\epsilon_{\text{eff}} + 1)^2}} = 0. \tag{14}$$

Thus, by knowing the absolute value of the reflection coefficient, one is able to estimate the effective relative permittivity by numerically solving (14). The absolute value of the reflection coefficient is calculated by simulating wave propagation in structure with an FDTD method. The FDTD method is a time-domain method, which means that reflected voltage is obtained as a function of time. The resulting time series is Fourier transformed to frequency domain. Only the lowest frequency points of the transformation are used to determine effective permittivity. In this way, we get a quasistatic solution that is valid when the radius of inclusion is much smaller than wavelength. Within the Rayleigh scattering approximation [17], the imaginary part of the effective permittivity of a lossless mixture is proportional to the third power of product of wave number and scatterer size

$$\Im\{\epsilon_{\text{eff}}\} \sim (k_0 a)^3. \tag{15}$$

Because the wavelength is much larger than the scattering particles, we ignore scattering. The transcendental equation is solved iteratively for effective permittivity with bisection method [18].

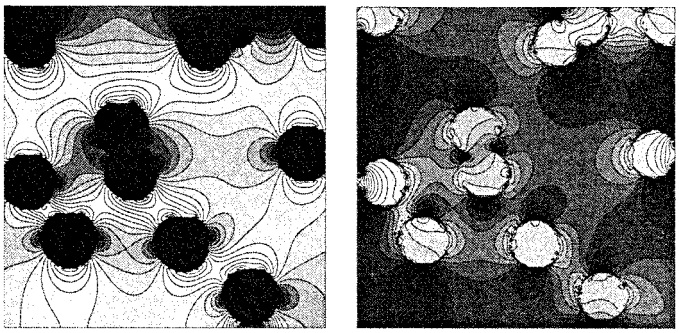

(a) Raisin pudding ($\epsilon_i = 16, \epsilon_e = 1$)

(b) Swiss cheese ($\epsilon_i = 1, \epsilon_e = 16$)

Fig. 2. Total electric field amplitude detected during low frequency simulation.

This method finds a value near the point in which the sign of the left-hand side of (14) is changed.

The technique is described more accurately in our earlier publication [1]. In this paper, however, the permittivity values for computation lattice were calculated with the technique introduced by Kaneda, Houshmand, and Itoh [19]. When computation domain size is 300 × 100 cells and 32 768 time steps are calculated, one simulation takes about 7.5 min to carry out with a PII 400 MHz PC processor.

V. Results

All results in this paper are calculated for two-phase mixtures having permittivity contrast 16. We treat two types of mixtures: raisin pudding, where the inclusion permittivity is higher than the environment permittivity ($\epsilon_i > \epsilon_e$), and Swiss cheese, an inverted mixture where the inclusion permittivity is lower than the environment permittivity ($\epsilon_i < \epsilon_e$). The computation domain size is $0.75\,\text{m} \times 0.25\,\text{m}$ ($d = 0.25$ m, $w = 0.25$ m, of Fig. 1). These two types of mixtures have drastically different field distributions, as illustrated for two samples in Fig. 2. There, the contour plots of the electric field amplitude in low frequency simulation is plotted. Also, the positions of inclusions can be clearly seen. As expected, the field amplitudes are smaller in areas where the permittivity is higher. Hence, in the raisin pudding mixture, the electric field is attenuated inside inclusions, while in the case of inverted mixture, there is an increase in field strength.

A. Bounds

In Fig. 3, one can see the effective permittivities achieved from 1000 simulations for raisin pudding. In every simulation, both the volume fraction and positioning of inclusions were randomly chosen. Therefore, the calculated effective permittivities are distributed to the area between the Wiener bounds. No sample can fall outside those absolute limits. Of course, it is possible that a sample can give a permittivity of Wiener limit, but that is very unlikely to happen. It would mean that all the inclusions form linear clusters in the horizontal or vertical direction. In fact, that type of situation was experimented with just to test FDTD-algorithm. Instead of a mixture sample, a number of straight inclusion walls were modeled. Simulation results were in very good agreement with the Wiener limits.

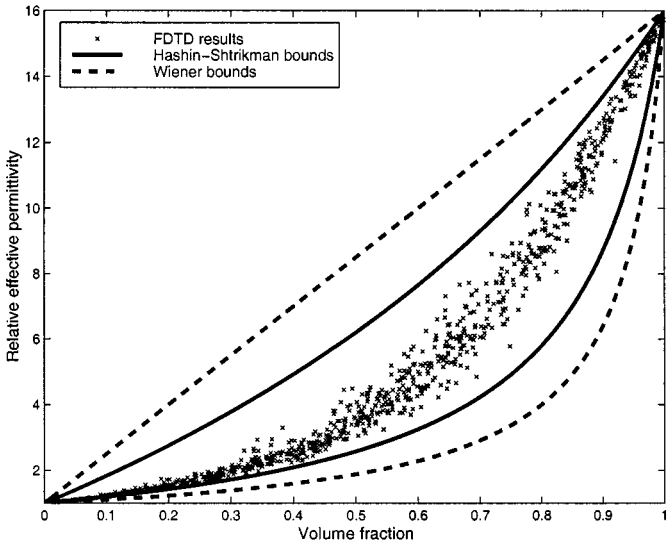

Fig. 3. Effective permittivities of random raisin pudding mixtures ($\epsilon_i = 16, \epsilon_e = 1$) compared with theoretical bounds.

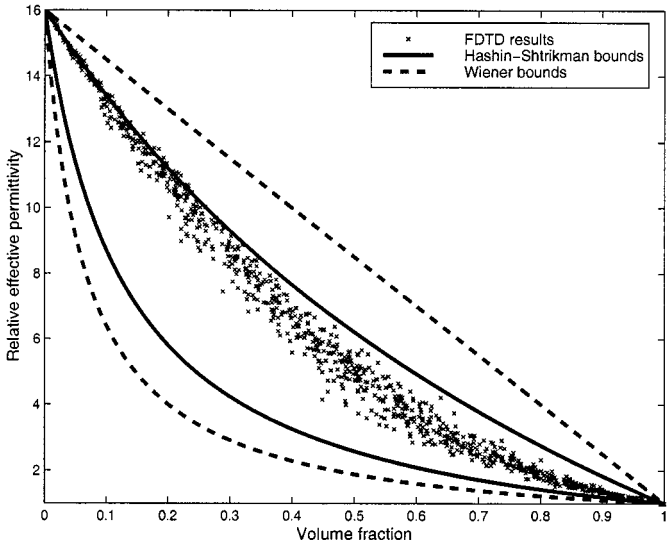

Fig. 4. Effective permittivities of random Swiss cheese mixtures ($\epsilon_i = 1$, $\epsilon_e = 16$) compared with theoretical bounds.

In Fig. 3, Hashin-Shtrikman bounds are also shown. It can be seen that the effective permittivity of random mixture lies almost always between those bounds. In Fig. 4, one can see corresponding plot for inverted mixture, and the simulation results here also fall mainly between the theoretical limits.

At certain volume fractions, the mixture simulations compose a distribution. The distribution derived from 3600 simulations at volume fraction 0.5 can be seen in Fig. 5 as a histogram. The distribution is calculated for an inverted mixture. The shape of distribution seems to be rather close to Gaussian distribution with mean value 4.80 and standard deviation 0.437.

From this large set of 3600 mixtures, we chose the samples with minimum and maximum effective permittivity values. The microgeometry of those samples is shown in Fig. 6. It can be

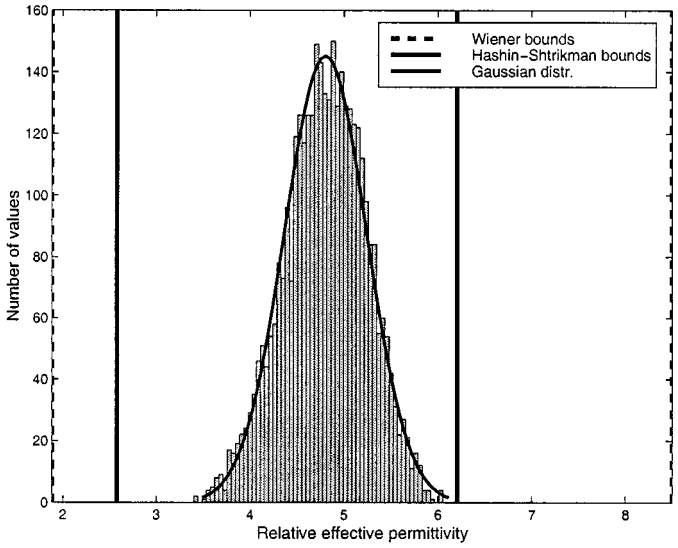

Fig. 5. The distribution of effective permittivities derived from 3600 simulations for Swiss cheese mixtures having volume fraction 0.5 ($\epsilon_i = 1$, $\epsilon_e = 16$). The mean value is 4.80 and standard deviation is 0.437.

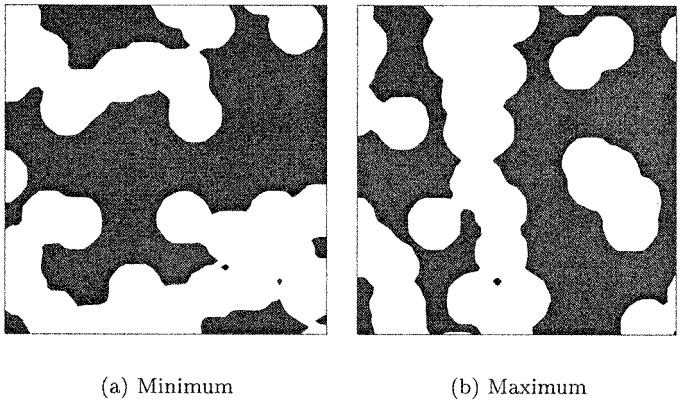

Fig. 6. Mixture samples that offered minimum and maximum permittivities in the distribution of Fig. 5 (a set of 3600 samples). Dark color stands for environment $\epsilon_e = 16$ and white for inclusions $\epsilon_i = 1$.

clearly seen that in samples offering minimum permittivity inclusions form clusters in the horizontal direction (perpendicular to electric field polarization of TEM mode). The sample with maximum permittivity inclusions forms clusters in the vertical direction (parallel to electric field polarization of TEM mode). This is very natural, because in theory, the absolute minimum or maximum value of mixture permittivity is achieved with the inclusions, which are actually plates in the horizontal or vertical direction.

B. Mixing Models

In Figs. 7 and 8, the set of 1000 FDTD simulation results is compared with general theoretical models of (3). Of the well-known formulas that the model contains, the Bruggeman model appears to be closest to the numerical results. But it should be noticed that not any single value of ν provides globally good agreement with FDTD simulations. However, with ν-value circa 0.7, the model is optimum in the case of raisin pudding, while

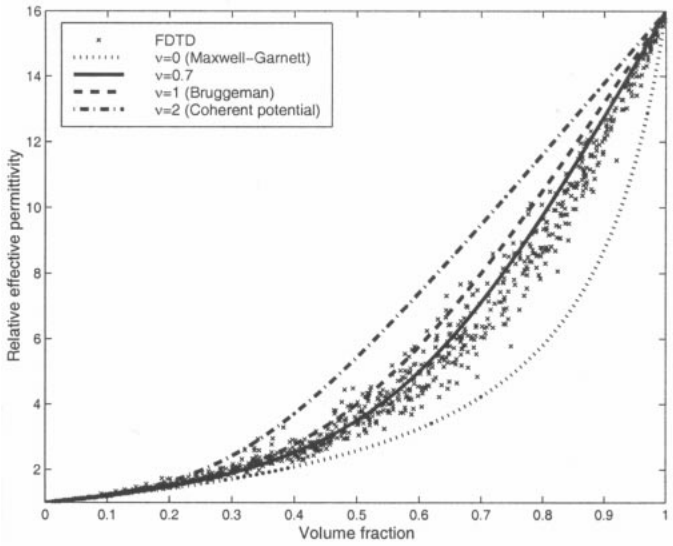

Fig. 7. Simulated FDTD results of raisin pudding mixtures compared with the ν-models calculated from (3).

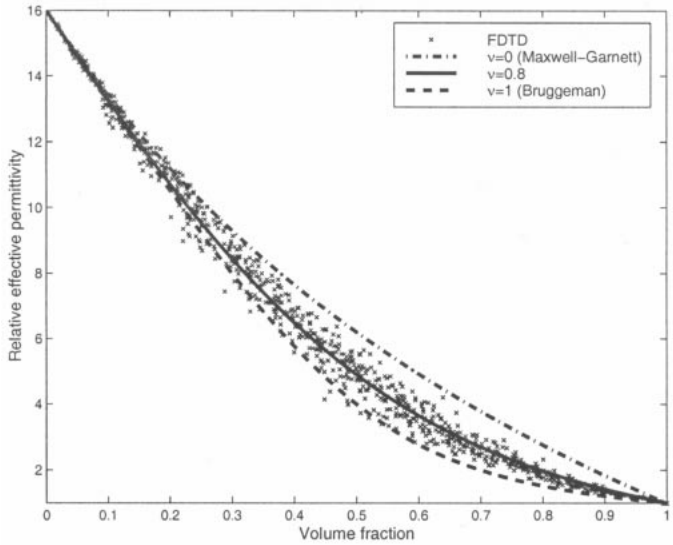

Fig. 8. Simulated FDTD results of Swiss cheese mixtures compared with the ν-models calculated from (3).

$\nu = 0.8$ provides reasonably good results in the case of inverted mixture.

In Figs. 9 and 10, a few exponential model curves are plotted along with the FDTD results. As in the case of ν-models, it is seen that no single exponential model can provide good prediction for the full range of volume fraction $(0 \ldots 1)$. If β-value is fitted so that that model agrees well in low volume fractions, the model predicts poor results at high volume fraction values and vice versa. On the average, rather low β values show the best fit. Of the used exponential models, $\beta = -0.1$ seems to agree best with the raisin pudding simulations, and for the Swiss cheese mixture, $\beta = 0.2$ might be a reasonable choice. This is studied in detail in Fig. 11. A sixth-order polynomial curve is fitted to the FDTD data in the least squares sense. Fig. 11 shows the relative difference of the ν and β models, and the nonglobal validity of the models can be observed.

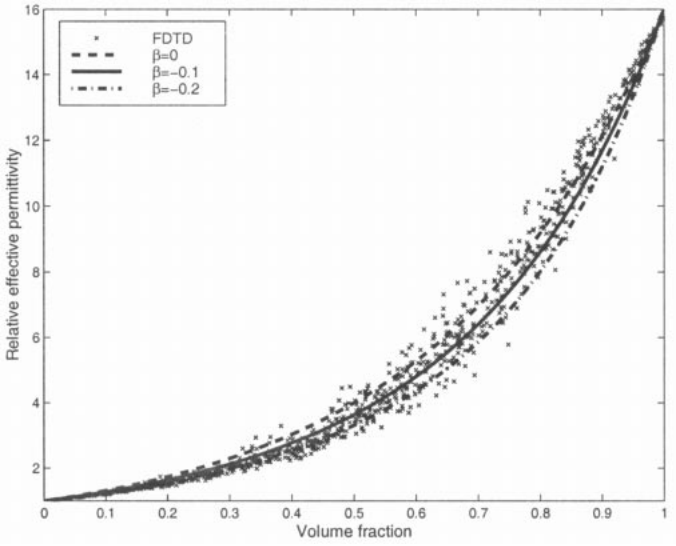

Fig. 9. Simulated FDTD results of raisin pudding mixtures compared with the exponential models calculated from (4).

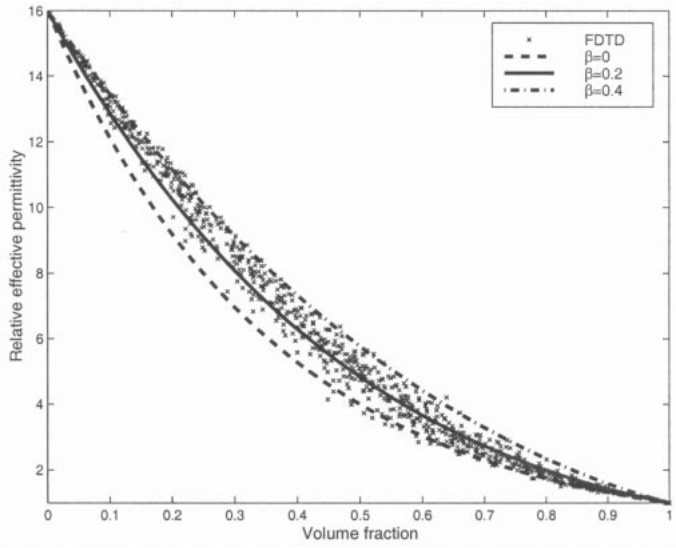

Fig. 10. Simulated FDTD results of Swiss cheese mixtures compared with the exponential models calculated from (4).

VI. Accuracy of Algorithm

In the numerical permittivity determination, reflection coefficients of frequencies below 26 MHz were used. The cutoff frequency of the simulated waveguide is circa 600 MHz. Random mixture samples generate a theoretically infite number of modes, but every higher mode is exponentially damped along the waveguide at the frequencies below cutoff. The attenuation factor for the first mode above TEM is [20]

$$\alpha = \Im\left\{\sqrt{\omega^2\mu_0\epsilon_0 - \left(\frac{\pi}{d}\right)^2}\right\} = 12.6\,\frac{1}{\mathrm{m}} \qquad (16)$$

at 26 MHz. In simulations, the reflected voltage was observed at 0.25 m from the mixture. Therefore, at that distance, this second lowest mode is attenuated 28 dB. But of course, the error is much smaller than this, because very little of the power is transformed to the reactive field of second lowest mode. And higher modes

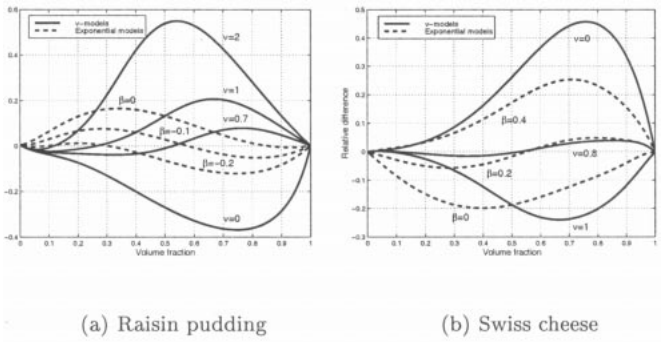

Fig. 11. Relative difference between mixing models and curve fitted to FDTD data as a function of inclusion volume fraction.

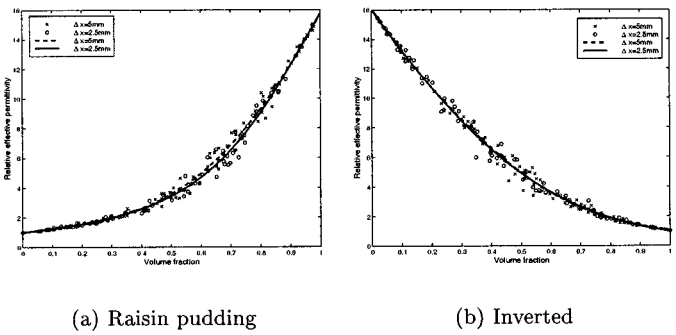

Fig. 12. Effect of the grid size $\Delta x = 5$ mm and $\Delta x = 2.5$ mm on the calculated permittivities of the samples. A sixth-order polynomial is fitted to the data set for both grid sizes.

are damped even more heavily. Hence, at the frequencies below 600 MHz, the only possible way the power can escape is basic TEM mode. The mixture slab acts like a resonator that has reactive fields close to it. Finally, because of lossless material, all the field power is transformed back to TEM mode and escapes through absorbing boundaries.

However, to test the effect of higher-order modes, ten random mixtures were also calculated with a longer waveguide such that the reflected voltage was observed at 0.5 m from the mixture slab. The result was that these simulations gave practically the same results as in the case of the smaller computation domain. In all ten cases, the calculated effective permittivity difference was less than 0.04%. Therefore, it can be argued that 0.25 m is far enough from mixture to measure voltage.

In calculations, the absorbing boundary was Mur's first-order boundary condition [21]. This very simple absorbing boundary is useful in this case, because it is fast and very efficient for waves that come perpendicularly to boundary. Also, Berenger's PML [22] with 16 layers was experimented with, and it was found that results always diverged less than 0.5%.

The largest error source seems to be the roughness of the grid when modeling circular inclusions. This problem turns out to be more severe in the case of the raisin pudding mixture than in the inverted mixture. The effect of the grid size was studied next. One hundred simulations were run with twice denser ($\Delta x = 2.5$ mm) computation mesh than what we normally used ($\Delta x = 5.0$ mm). A polynomial, sixth-order curve is fitted to these data. The corresponding curve in case of normal gridsize is also calculated for comparison. Fig. 12 illustrates this comparison. It

can be seen that in the case of the raisin pudding mixture, average results decrease slightly when grid size is reduced (i.e., the field is calculated more accurately). But in case of the inverted mixture, this trend cannot be seen. Therefore, in simulations of raisin pudding mixtures, this denser mesh ($\Delta x = 2.5$ mm) was used for all results, and in the case of the Swiss cheese mixture, the coarser mesh $\Delta x = 5.0$ mm was used in order to optimize the speed of simulation.

VII. Conclusion

For this paper, we have run thousands of FDTD simulations to get a good picture of the average characteristics of random dielectric mixture. One should always remember that no one of the mixing models could offer the absolute truth for a certain volume fraction, because in random mixtures, all values between Wiener limits are possible. Instead, we can try to predict the most likely value for effective permittivity. Mixture samples with randomly positioned inclusions build a probability distribution for effective permittivity. However, it is very probable that a mixture with a large number of inclusions is almost isotropic and therefore, Hashin-Shtrikman bounds seem to offer reasonable limits. When looking at Figs. 3 and 4, one might even consider more strict bounds. But it is difficult to derive bounds or mixing models based on the FDTD results, because then we should also study the number of different permittivity contrasts. In this paper, only one contrast was studied.

References

[1] O. Pekonen, K. Kärkkäinen, A. Sihvola, and K. Nikoskinen, "Numerical testing of dielectric mixing rules by FDTD method," *J. Electromagn. Waves Applicat.*, vol. 13, pp. 67–87, 1999.

[2] L. Greengard and M. Moura, "On the numerical evaluation of electrostatic fields in composite materials," *Acta Numerica*, pp. 379–410, 1994.

[3] B. Sareni, L. Krähenbühl, A. Beroual, and C. Brosseau, "Effective dielectric constant of periodic composite materials," *J. Appl. Phys.*, vol. 80, no. 3, pp. 1688–1696, 1996.

[4] B. Sareni, L. Krähenbühl, A. Beroual, and C. Brosseau, "Effective dielectric constant of random composite materials," *J. Appl. Phys.*, vol. 81, no. 5, pp. 2375–2383, 1997.

[5] J. C. M. Garnett, "Colors in metal glasses and metal films," *Trans. Roy. Soc.*, vol. 53, pp. 385–420, 1904.

[6] A. Sihvola and I. Lindell, "Polarizability modeling of heterogeneous media," in *Dielectric Properties of Heterogeneous Materials, PIER 6 Progress in Electromagnetics Research*, A. Priou, Ed. New York: Elsevier, 1992, pp. 101–151.

[7] D. A. G. Bruggeman, "Berechnung verschiedener physikalischer konstanten von heterogenen substanzen, i. dielektrizitätskonstanten und leitfähigkeiten der mischkörper aus isotropen substanzen," *Ann. Phys.*, pp. 636–664, 1935.

[8] D. Polder and J. H. van Santen, "The effective permeability of mixtures of solids," *Physica*, vol. 12, no. 5, pp. 257–271, 1946.

[9] A. Sihvola, "Self-consistency aspects of dielectric mixing theories," *IEEE Trans. Geosci. Remote Sensing.*, vol. 27, pp. 403–415, July 1989.

[10] R. J. Elliott, J. A. Krumhansl, and P. L. Leath, "The theory and properties of randomly disordered crystals and related physical systems," *Rev. Mod. Phys.*, vol. 46, pp. 465–543, July 1974.

[11] W. E. Kohler and G. C. Papanicolaou, "Some applications of the coherent potential approximation," in *Multiple Scattering and Waves*, P. L. Kohler and G. C. Papanicolaou, Eds. New York: North Holland, 1981, pp. 199–223.

[12] J. R. Birchak, L. G. Gardner, J. W. Hipp, and J. M. Victor, "High dielectric constant microwave probes for sensing soil moisture," *Proc. IEEE*, vol. 62, pp. 93–98, Jan. 1974.

[13] H. Looyenga, "Dielectric constants of mixtures," *Physica*, vol. 31, pp. 401–406, 1965.

[14] K. Lichtenecker and K. Rother, "Die herleitung des logarithmischen mischungsgesetzes aus allgemeinen prinzipien der stationären strömung," *Phys. Zeitschr.*, vol. 32, pp. 255–260, 1931.

[15] O. Wiener, "Zur theorie der refraktionskonstanten," *Berichteüber Verhandlungen Königlich-Sächsischen Gesellschaft Wisseschaften Leipzig*, pp. 256–277, 1910.

[16] Z. Hashin and S. Shtrikman, "A variational approach to the theory of the effective magnetic permeability of multiphase materials," *J. Appl. Phys.*, vol. 33, no. 10, pp. 3125–3131, 1962.

[17] D. R. Huffman and C. F. Bohren, *Absorption and Scattering of Light by Small Particles*: Wiley, 1983.

[18] K. E. Atkinson, *An Introduction to Numerical Analysis*. New York: Wiley, 1988, ch. 2.

[19] N. Kaneda, B. Houshmand, and T. Itoh, "Fdtd analysis of dielectric resonators with curved surfaces," *IEEE Trans. Microw. Theory Tech.*, vol. 45, pp. 1645–1648, Sept. 1997.

[20] R. E. Collin, *Foundations for Microwave Engineering*. New York: McGraw-Hill, 1966, ch. 3.

[21] G. Mur, "Absorbing boundary conditions for the finite-difference approximation of the time-domain electromagnetic-field equations," *IEEE Trans. Electromagn. Compat.*, vol. EMC-23, no. 4, pp. 377–382, 1981.

[22] J.-P. Berenger, "A perfectly matched layer for the absorption of electromagnetic waves," *J. Comput. Phys.*, vol. 114, no. 1, pp. 185–200, 1994.

Kimmo Kalervo Kärkkäinen was born on February 1, 1973, in Kuopio, Finland. He received the Diploma Engineer degree in electrical engineering from Helsinki University of Technology (HUT), Espoo, Finland, in 1998.

He is now doing his postgraduate studies and working as a Researcher with the Electromagnetics Laboratory, HUT. His main research interests include electromagnetic theory, numerical methods, and especially FDTD techniques.

Ari Henrik Sihvola was born on October 6, 1957, in Valkeala, Finland. He received the degrees of Diploma Engineer, Licentiate of Technology, and Doctor of Technology, all in electrical engineering, all from the Helsinki University of Technology (HUT), Espoo, Finland, in 1981, 1984, and 1987, respectively.

Besides working for HUT and the Academy of Finland, he was a Visiting Engineer, Research Laboratory of Electronics, Massachusetts Institute of Technology (MIT), Cambridge, from 1985 to 1986. From 1990 to 1991, he was a Visiting Scientist with the Pennsylvania State University, State College. In 1996, he was a Visiting Scientist with Lund University, Lund, Sweden. He is now a Professor of Electromagnetics with HUT, with interests in electromagnetic theory, complex media, remote sensing, and radar applications.

Dr. Sihvola is Vice Chairman of the Finnish National Committee of URSI (International Union of Radio Science). He also served as the Secretary of the 22nd European Microwave Conference, Espoo, Finland, 1992.

Keijo I. Nikoskinen was born in Kajaani, Finland in 1962. He received the Dipl.Eng., Lic.Tech., and Dr.Tech. degrees, all in electrical engineering, from Helsinki University of Technology (HUT), Espoo, Finland, in 1986, 1989, and 1991, respectively.

From 1991 to 1994, he was a Junior Scientist with the Academy of Finland. He is currently a Professor of Electromagnetics with HUT. His main professional interests are computational methods of electromagnetic field theory and antenna applications.